Conf-940933--38

UCRL-JC-117107
PREPRINT

Scrape-off Layer Plasma Modeling for the DIII-D Tokamak

G. D. Porter, T. D. Rognlien, S. L. Allen, M. D. Brown, R. B. Campbell, R. H. Cohen, G. G. Craddock, H. E. Dalhed, P. H. Diamond, M. E. Fenstermacher, R. W. Harvey, D. N. Hill, R. A. Jong, D. A. Knoll, A. E. Koniges, K. Kupfer, T. W. Leonard, L. L. LoDestro, D. L. Marcus, M. A. Mahdavi, N. Mattor, J. L. Milovich, W. H. Meyer, J. M. Moller, M. E. Rensink, D. D. Ryutov, H. A. Scott, G. R. Smith, R. D. Stambaugh, A. S. Wan, X. Xu

This paper was prepared for
15th IAEA International Conference
on Plasma Physics
and Controlled Nuclear Fusion Research
Madrid, Spain
September 26 - October 1, 1994

September 1994

Lawrence Livermore National Laboratory

This is a preprint of a paper intended for publication in a journal or proceedings. Since changes may be made before publication, this preprint is made available with the understanding that it will not be cited or reproduced without the permission of the author.

MASTER

DISTRIBUTION OF THIS DOCUMENT IS UNLIMITED

DISCLAIMER

This report was prepared as an account of work sponsored by an agency of the United States Government. Neither the United States Government nor any agency thereof, nor any of their employees, make any warranty, express or implied, or assumes any legal liability or responsibility for the accuracy, completeness, or usefulness of any information, apparatus, product, or process disclosed, or represents that its use would not infringe privately owned rights. Reference herein to any specific commercial product, process, or service by trade name, trademark, manufacturer, or otherwise does not necessarily constitute or imply its endorsement, recommendation, or favoring by the United States Government or any agency thereof. The views and opinions of authors expressed herein do not necessarily state or reflect those of the United States Government or any agency thereof.

DISCLAIMER

Portions of this document may be illegible in electronic image products. Images are produced from the best available original document.

Scrape-off Layer Plasma Modeling for the DIII-D Tokamak

G.D. Porter, T.D. Rognlien, S.L. Allen, M.D. Brown,

R.B. Campbell[1],R.H. Cohen, G.G. Craddock. H.E. Dalhed, P.H. Diamond[2],

M.E. Fenstermacher, R.W. Harvey[3], D.N. Hill, R.A. Jong, D.A. Knoll[4],

A.E. Koniges, K. Kupfer[3], T.W. Leonard[3], L.L. LoDestro, D.L. Marcus,

M.A. Mahdavi[3], N. Mattor, J.L. Milovich, W.H. Meyer, J.M. Moller,

M.E. Rensink, D.D. Ryutov[5], H.A. Scott, G.R. Smith, R.D. Stambaugh[3],

A.S. Wan, X. Xu

Lawrence Livermore National Laboratory

[1] Sandia National Laboratory-NM

[2] University of California, San Diego

[3] General Atomics

[4] Idaho National Engineering Laboratory

[5] On leave from Budker Institute of Nuclear Physics, Novosibirsk, Russia

Scrape-off Layer Plasma Modeling for the DIII-D Tokamak*

Abstract

The behavior of the scrape-off layer (SOL) region in tokamaks is believed to play an important role determining the overall device performance. In addition, control of the exhaust power has become one of the most important issues in the design of future devices such as ITER and TPX. This paper presents the results of application of 2-D fluid models to the DIII-D tokamak, and research into the importance of processes which are inadequately treated in the fluid models. Comparison of measured and simulated profiles of SOL plasma parameters suggest the physics model contained in the UEDGE code is sufficient to simulate plasmas which are attached to the divertor plates. Experimental evidence suggests the presence of enhanced plasma recombination and momentum removal leading to the existence of detached plasma states. UEDGE simulation of these plasmas obtains a bifurcation to a low temperature plasma at the divertor, but the plasma remains attached. Understanding the physics of this detachment is important for the design of future devices. Analytic studies of the behavior of SOL plasmas enhance our understanding beyond that achieved with fluid modeling. Analysis of the effect of drifts on sheath structure suggest these drifts may play a role in the detachment process. Analysis of the turbulent-transport equations indicate a bifurcation which is qualitatively similar to the experimentally different

---

* This work supported by the USDOE under contracts W-7405-ENG-48 at LLNL, DEA-C093-89ERS51114 at General Atomics, DE-FG03-88ER53275 at UCSD, AC07-76ID01570, at INEL, and DE-AC04-94AL85000 at SNL-NM.

behavior of the L- and H-mode SOL. Electrostatic simulations of conducting wall modes suggest possible control of the SOL width by biasing.

1. UEDGE Code Validation Results

Fluid SOL codes must be validated against data from present diverted tokamaks to demonstrate their applicability. The validated codes can then be used to design future divertor configurations. We report the results of UEDGE[1] code validation against data from the DIII-D tokamak here. Application of the code to divertor design has been described by Fenstermacher[2]. The SOL of DIII-D is well diagnosed to determine the relevant plasma parameters at several poloidal locations. The electron density (n_e) and temperature (T_e) are measured by Thomson scattering, a retractable Langmuir probe array near the mid plane (Z=0), and a Langmuir probe array which spans the lower divertor. The ion temperature (T_i) is determined by Charge Exchange Recombination (CER) at $Z \approx 0$. The power deposited on the divertor floors and the center post is measured with Infrared camera systems (IRTV). Hydrogen recycling is measured by observing H_α emission with both photo diode arrays, and TV systems. Data from these diagnostics are compared with simulations using the UEDGE code for H-mode (both ELM-free and ELMing), and L-mode plasmas. UEDGE assumes classical physics for energy and particle transport along the magnetic field **B**, and anomalous transport across **B**.

Perpendicular transport coefficients for thermal energy are adjusted to obtain consistency with T_e and T_i profiles measured near the outer mid plane of DIII-D. We find $0.1 \leq \chi_e \leq 0.3$ m^2/s for H-mode, and up to an order of magnitude larger for L-mode. The experimentally measured T_i in the SOL is higher than T_e, and the radial scale length of the variation of T_i is longer than that of T_e. We find it necessary to set $\chi_i > \chi_e$ to simulate the measured profiles,

with H-mode ion thermal transport coefficients up to 1 m^2/s. We find that both χ_i and χ_e increase roughly linearly with neutral beam heating power for fixed plasma current.

The perpendicular particle transport coefficient , $D_\perp$, is varied to obtain consistency with the measured density profile. The determination of this coefficient is more problematic than that of the thermal transport coefficients because of the uncertainty in the particle flux into the SOL. The upstream radial profile of the density is determined by a combination of $D_\perp$ and the particle recycling coefficient at the divertor floor, R_P. In steady state, the particle throughput in the simulation is determined by the assumed particle removal rate, i.e., by R_P and the neutral particle albedo at the outer wall. We estimate the particle throughput from the rate of rise of the core density at the L- to H-mode transition. The measured density rise implies a source rate in the range of 100–300 $T \cdot \ell/s$ at the L- to H-mode transition. At steady state, we expect the particle flux into the SOL to be similar to this source rate. We obtain consistency between these estimates of the particle throughput and simulations with $0.05 \leq D_\perp \leq 0.25$ m^2/s, and $0.975 \leq R_P \leq 0.985$ for H-mode plasmas. We find that $D_\perp$ increases with neutral beam heating power, and is roughly a factor of 4–5 higher in L-mode than in H-mode.

The effect of impurity radiation in the SOL can be modeled in several ways with the UEDGE code, including multi-species fluid modeling[3]. To date, we have used a constant impurity density fraction to model the effect of impurities in our detailed code validation effort. The radiated power uses emission rates which take into account finite impurity lifetime and charge exchange recombination with the hydrogenic neutrals. We find that a Carbon impurity fraction of 0.5% to 1.0% is sufficient to provide radiated power consistent with that measured on bolometer arrays on DIII-D.

We have also used force-balance impurity transport models to study the effects of Carbon and Neon flows for parameters similar to DIII-D. Simulations in 2-D show enhanced impurities at the midplane due to radial transport and flow reversal compared to 1-D simulations that only include parallel friction and thermal force effects. Carbon radiation concentrates near the divertor plate, while Neon radiation is spread throughout the SOL.

The simulated plasmas obtained with the transport coefficients and impurity fractions described above are consistent with other experimental data: the total power flowing across the separatrix; the amplitude and shape of the heat flux profile at the outer strike point of single null configurations; and the intensity of H_α emission near both the inner and outer divertor strike points. The measured and simulated profiles of heat flux and Lyman-α emission are shown in Fig. 1. The consistency between experiment and model which has been obtained to date provides confidence in the applicability of UEDGE to DIII-D divertor design.

2. Simulation of Experimentally Detached Plasmas

The simulations of DIII-D plasmas described in the previous section typically indicate power and ion current to the inner strike point which are much larger than that measured. We find that the introduction of impurity radiation reduces the power to the inner plate more than to the outer because of the inherently lower temperature and higher density at the inner plate. Indeed, when impurity radiation is introduced in the code we obtain a thermally collapsed solution with T_e less than 1 eV at the inner plate. Collapse is often associated with a bifurcation in the solution where three solutions can exist for the same parameters; two being stable, and one unstable. The plasma pressure is roughly constant along a flux surface, hence there is a high plasma density in the region of low T_e. There is a high ion current to the inner plate

because of recycling. Most of the simulated power to the inner plate arises from recombination of the ions in the plate. In contrast, the ion current measured by Langmuir probes is low, and the electron pressure at the inner plate is on the order of 50 times lower than that measured at the mid plane or at the outer plate. This experimental state is referred to as a detached plasma.

Experimentally, we typically observe this detached state at the inner divertor plate, and a corresponding low divertor power. The addition of gas, either hydrogen or impurity, leads to detachment at the outer strike point in the experiment, although the plasma remains attached at larger radii. We obtain a thermally collapsed plasma state at the outer strike point in the UEDGE simulation of these plasmas when we add gas injection similar to that used in the experiment. We believe there is a relation between the simulated collapsed state, and the experimentally observed detached state. As in the experiment, the poloidal location of the gas puff is relatively unimportant. The peak heat flux is reduced by a factor of two, similar to the experiment. However, the plasma density is at least a factor of 10 higher than seen experimentally. An upper-bound model where each charge-exchange collision removes all of the ion drift momentum, reduces the density by only a factor of 2. Initial calculations with carbon radiation reduces the density further. The experimental results suggest the existence of a recombination process which is faster than the radiative and three body processes used in the simulation. The observation of a reduction in the plasma pressure seen in the experiment also suggests an enhanced momentum removal rate.

3. Extended analysis of SOL physics

We consider several theoretical issues to better understand the underlying physics mechanisms and to improve transport code models.

The aforementioned disparity in transport coefficients (and the corresponding disparity in SOL widths) between L- and H-mode may be related to a bistable property of the coupled turbulence-transport equations. As the SOL T_e width Δ is decreased, the minimum radial mode number increases, increasing the polarization response. This, in conjunction with energy end loss, tends to decrease the growth rate and mixing-length diffusivity for modes driven by plasma rotation, curvature, or a combination, and for small-enough Δ, this effect dominates over the increased instability drive. This is illustrated in Fig. 2 for a point model of DIII-D. The equilibrium points Q=P are stable (unstable) for $dQ/d\Delta < (>) 0$. For still smaller Δ, some other transport mechanism (here, a simple model for $dv_{\parallel}/dr$-driven turbulence) provides a second stable root. For the wider stable root, radial transport from curvature- and rotation-driven turbulence balances end loss, as discussed in [4]. We speculate that the SOL selects between these roots based on boundary conditions at the separatrix, which tends to favor the narrow root in H and VH modes, and the broad root in L and OH modes. We are testing this conjecture by running UEDGE with the same mixing-length transport coefficients used to construct Fig. 2.

Linear stability analysis of the ionization front of a thermally collapsed and/or detached plasma state indicate that the radiative condensation instability, familiar from astrophysical calculations, is important in forming a MARFE-like solution. In addition, a perturbation of this front, such as would be expected from an ELM, could excite a Richtmeyer-Meshkov instability which will reconnect the plasma to the divertor plate. Other instabilities which may play a role in the formation of a detached state include Rayleigh-Taylor mode driven by braking forces parallel to **B**, and in the direction of decreasing

density; and a Kelvin-Helmoltz instability resulting from the interaction of the toroidally rotating plasma interfacing with a dense divertor plasma.

Analytical studies of drift wave mode structure near an X-point indicate that standard "flute ordered" eikonal expansions break down in such regions. Analysis using a full 3-D mode equation in X-point geometry indicates the rays deviate significantly from "flute-ordered" behavior, and the amplitude is greatly diminished near the X-point, suggesting small perpendicular transport in that region.

A series of 2-D electrostatic simulations of the conducting-wall mode have been done to analyze both RF biasing of the divertor plate to broaden the SOL and effects of radially sheared drift velocity. Resonant biasing of $e\phi_{bias}/T_e=0.5$ doubles the radial heat flux. The $\mathbf{E}\times\mathbf{B}$ drift profile resulting from close coupling of the equilibrium ϕ and T_e in the SOL reduces the turbulence flux by 71% and the root mean square magnitude of fluctuating density by 31%. However, in the case of negative biasing with $e\phi_{bias}/T_e=-3$, the velocity shear increases the turbulence flux by 230% and the root mean square fluctuating density by 36%.

We consider the effect of drifts on sheath structure and flows for a toroidal limiter or poloidal divertor. A current produced by the $\mathbf{E}\times\mathbf{B}$ drift across the sheath and the accompanying density asymmetry produces an appreciable parallel current through the SOL. When $v_{E\times B} > c_s \sin\theta$, where θ is the angle between $\mathbf{B}$ and the plates, the plasma nearly detaches from one plate. The diamagnetic drifts do not affect the sheath current-voltage characteristics and do not contribute to the asymmetries of the plasma flow to the plates. The closing of the electron diamagnetic current occurs by its transformation (within the sheath) into the parallel electron current. If the θ's at opposite ends of a field line are not properly mutually adjusted, then the

conditions for closing of the electron currents on the opposite plates don't match each other, giving rise to electron convection.

The thermally collapsed plasma with high neutral-density near the divertor plate is optically thick to the line radiation and results in reduced power fluxes to the divertor plate. We use the CRETIN[5] code to model hydrogen radiation transport for UEDGE simulations of DIII-D gas-puff parameters, and find the Lyman-α line is strongly re-absorbed. Ignoring the reabsorption of the line radiation results in significant over-estimates of the hydrogen radiation flux to the divertor plate.

A three-dimensional (distance along the field + 2-v) Fokker-Planck code[6] is being used to determine the parallel electron heat flux for a plasma terminating on a wall. Work in progress includes comparison of the results with various analytic models, including one which specifically includes boundary effects[7].

References

[1] T.D. Rognlien, et.al., J. Nucl. Mat. **196-198** (1992) p. 347-351.

[2] M. E. Fenstermacher, et.al., UEDGE and DEGAS Modeling of the DIII-D Scrape-off Layer Plasmas, to be published in J. Nucl. Mat.

[3] G. R. Smith, et.al., Techniques and Results of Tokamak-Edge Simulation, to be published in J. Nucl. Mat.

[4] R.H. Cohen, N. Mattor, X. Xu, Contr. Plasma Phys. **34**, (1994) p. 232.

[5] A. S. Wan, H. E. Dalhed, H. A. Scott, D. E. Post, T. D. Rognlien, Detailed Radiative Transport Modeling of a Radiative Divertor, to be published in J. Nucl. Mat.

[6] O. Sauter, R.W. Harvey, F.L. Hinton, Contr. Plasma Phys. **34**, (1994) p. 169.

[7] R.H. Cohen, T.D. Rognlien, Contr. Plasma Phys. **34**, (1994) p. 198.

Figure Captions

Fig. 1: Comparison of the experimentally measured profiles of divertor power at the outer strike point (a), and H_α emission across the divertor floor (b) with UEDGE simulation.

Fig. 2: Mixing-length flux Q normalized to the power density P across the separatrix, vs. SOL width Δ. The temperature has been eliminated using power balance.

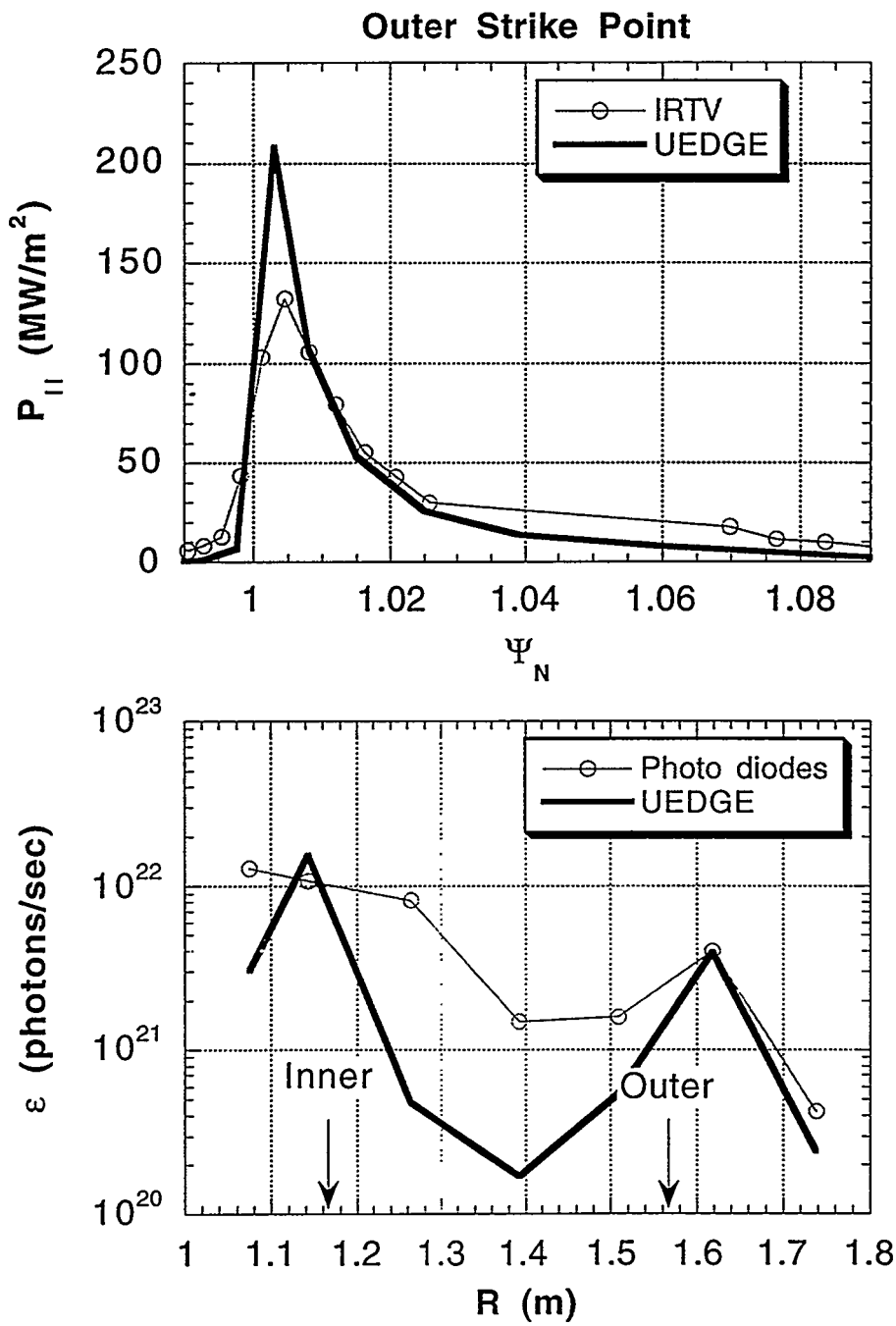
Outer Strike Point
IRTV
UEDGE
$P_{\parallel}$ (MW/m^2)
250
200
150
100
50
0
1
1.02
1.04
1.06
1.08
Ψ_N
Photo diodes
UEDGE
ε (photons/sec)
10^{23}
10^{22}
10^{21}
10^{20}
Inner
Outer
1
1.1
1.2
1.3
1.4
1.5
1.6
1.7
1.8
R (m)

Fig. 1

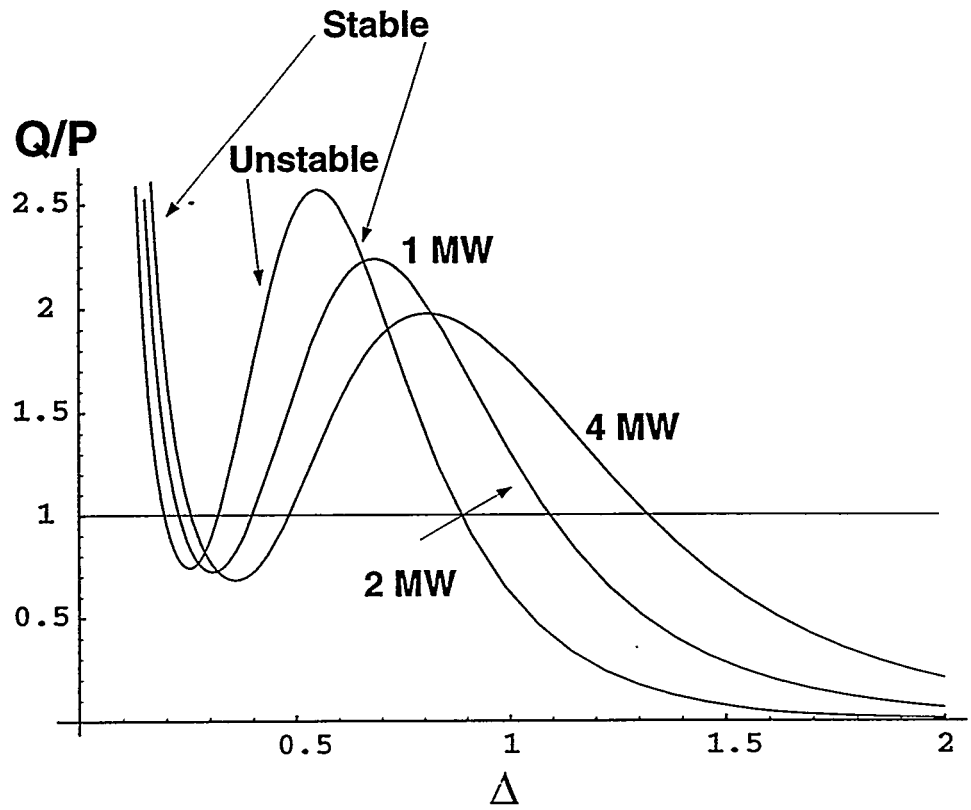

Fig. 2